Macromolecules

ARTICLE

pubs.acs.org/Macromolecules

A Detailed Investigation of the Free Radical Copolymerization Behavior of *n*-Butyl Acrylate Macromonomers

Anna-Marie Zorn,[†] Thomas Junkers,[*,‡] and Christopher Barner-Kowollik[*,†]

[†]Preparative Macromolecular Chemistry, Institut für Technische Chemie und Polymerchemie, Karlsruhe Institute of Technology (KIT), Engesserstr. 18, 76128 Karlsruhe, Germany

[‡]Institute for Materials Research (IMO), Polymer Reaction Design Group, Universiteit Hasselt, Agoralaan, Gebouw D, BE-3590 Diepenbeek, Belgium

Supporting Information

ABSTRACT: The free radical copolymerization of macromonomers with low molecular weight monomers represents a versatile tool for the formation of statistical copolymers featuring pendant side chains. In the current study *n*-butyl acrylate macromonomer (BAMM) has been synthesized via high temperature acrylate synthesis in a one-pot−one-step procedure and copolymerized with benzyl acrylate (BzA) as a comonomer up to 40% conversion in a free radical copolymerization with 1,1′-azobis(isobutyronitrile) (AIBN) as a source of radicals. The copolymers poly(BAMM)-*co*-poly(BzA) are fully characterized via size exclusion chromatography (SEC), nuclear magnetic resonance spectroscopy (NMR), and liquid adsorption chromatography at critical conditions (LACCC). The achievable molecular weight of the synthesized poly(BAMM)-*co*-poly(BzA) lies between 8000 and 77 000 g mol^{-1} with a polydispersity of 1.30−2.12. Calculated copolymer compositions from the integrals of the specific resonances H_{ar} and CH_2 of the BzA compared to CH_2 of the BAMM have been subjected to a (terminal model) Mayo−Lewis analysis, resulting in estimated reactivity ratios at ∼40% conversion of r_{BzA} = 2.46 and r_{BAMM} = 1.79, indicating a copolymer composition of F_{BA} < 0.65 for the copolymers derived from f_{BzA} > 0.9 up to a copolymer composition of F_{BA} > 0.9 for copolymers with a comonomer feed of f_{BzA} < 0.6. The poly(BAMM)-*co*-poly(BzA) have been analyzed under critical conditions of *n*-butyl acrylate (BA) on a normal phase column to obtain an image of the generated poly(BAMM)-*co*-poly(BzA).

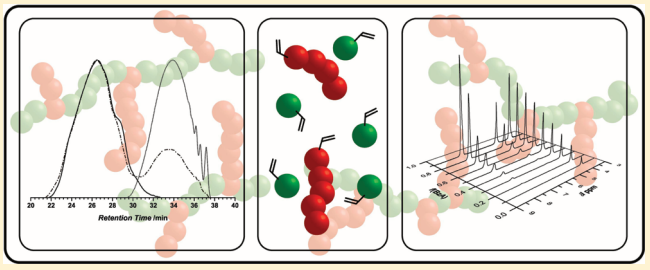

INTRODUCTION

Macromonomers are oligomeric or polymeric species with a polymerizable terminus.[1−5] Thus, they can constitute versatile synthetic building blocks and provide access to well-defined polymeric architectures such as branched polymers, block-, graft-, comb-, or star-polymers. Several synthetic pathways are conceivable for macromonomer formation.[6] Among others, polymers resulting from atom transfer radical polymerization (ATRP)[7] as a controlled radical polymerization method (CRP) have successfully been transformed into macromonomers via esterification or *click* chemistry[8,9] as well as addition−fragmentation chain transfer (AFCT) using various low molecular weight AFCT agents.[6] However, conventional free radical polymerization (FRP) techniques can also be employed to obtain polymers with high end group fidelity, albeit with higher polydispersity. Chiefari et al. introduced a macromonomer formation method based on the free radical polymerization of acrylates, which allows obtaining macromonomeric species in a one-pot synthesis.[10,11] During polymerization, the formation of macromonomers benefits from so-called midchain radicals (MCR).[12−14] These MCR undergo scission reactions at low monomer content and sufficiently high temperatures, resulting in vinyl-terminated species.[14] The reaction mechanism has been well-studied via detailed mass spectrometry analysis,[14−18] and detailed kinetic simulations were carried out to elucidate the limitations of macromonomer production in this approach.[19] Such a direct access route enables the synthesis of highly pure macromonomers via a one-pot−one-step procedure.[20] Our interest in simple access routes to vinyl-terminated polymers is driven by their applicability as versatile macromolecular building blocks for the assembly of complex polymer designs.[21] The terminal vinylic function can serve as a potentially powerful synthetic handle in copolymerization processes. Compared to other existing methods for macromonomer formation,[1,2,5,22] such a direct synthetic approach is very appealing as it does not require the use of specific control agents, postprocessing of polymers, and/or purification steps.

The vinyl terminus of the macromonomers can be employed in copolymerizations with a conventional monomer; this strategy represents an efficient pathway for constructing branched polymer architectures. Several research groups have employed free

Received: June 15, 2011
Revised: July 15, 2011
Published: August 04, 2011

Scheme 1. Synthesis of Copolymers via the Macromonomer Approach[a]

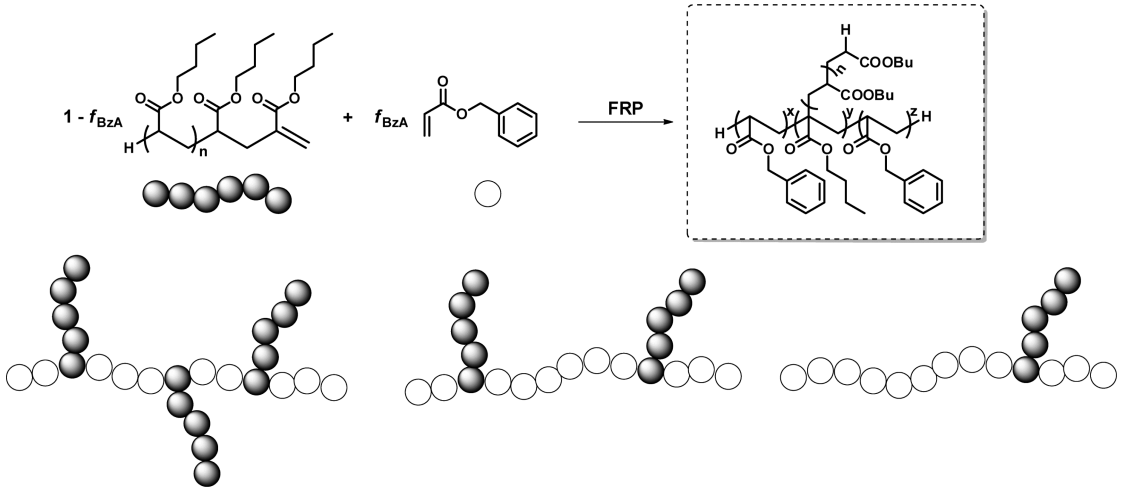

[a] BAMM was polymerized with benzyl acrylate (BzA) as a comonomer.

radical polymerization as well as living/controlled radical polymerization methods as ATRP and nitroxide-mediated polymerization (NMP) for the copolymerization of postfunctionalized macromonomers.[6,23−30]

In the current study we wish to report on the free radical copolymerization of macromonomers synthesized via the one-pot−one-step synthesis during high temperatures ($T \geq 140$ °C). We concentrate on *n*-butyl acrylate macromonomers (BAMM) copolymerized with benzyl acrylate (BzA) as a comonomer. Scheme 1 gives an overview of the synthetic route employed in the current study.

The copolymerization kinetics of a binary copolymerization mixture may be described in a simple approach via the so-called "terminal model", which only considers the terminal repeat unit of a propagating macroradical to be relevant for the copolymerization kinetics.[31] The so-called "penultimate unit effect model" was shown to be superior to the terminal model in the work of Fukuda et al.,[32] Davis et al.[33] and Coote et al.,[34,35] yet the terminal model remains an attractive "engineering-type" option for copolymer analysis. The penultimate model—in comparison to the terminal model—considers the penultimate units on the chain of the growing macroradicals. In the most copolymerizations the terminal model describes the composition data adequately, while a joint description of both rate and composition data often fails. The basis of the terminal model is represented by eq 1

$$R{-}M_i^{\bullet} + M_j \rightarrow R{-}M_i{}^{\bullet}M_j \qquad (1)$$

with k_{pij}, where i, j = 1 or 2. The reactivity ratios of the participating comonomers in the polymerization are defined as $k_{p11}/k_{p12} = r_1$ and $k_{p22}/k_{p21} = r_2$, respectively. Knowledge of the r values can be employed to determine the (instantaneous) copolymer composition in a binary system by the use of the Mayo−Lewis equation (5), which is described in more detail in the Results and Discussion section.

As an initial analysis method, size exclusion chromatography (SEC) was employed for the molecular weight determination of the generated copolymers. For the determination of the reactivity ratios via the copolymer composition ^{1}H NMR spectroscopy and integration of specific signals were utilized. However, conventional SEC analysis of copolymers gives an indication about the formation of high molecular weight species, but is not specified with regard to the composition of the copolymer in terms of block length of the comonomers and the ratio of secondarily build homopolymer, since homo- and copolymers of the same hydrodynamic volume cannot be distinguished. The use of liquid adsorption chromatography at critical conditions (LACCC), as an additional characterization method, can yield more detailed information. Thereby, the molecules are separated by their chemical heterogeneity in the absence of size exclusion effects. At critical conditions, which are located between the size exclusion chromatography (SEC) mode and liquid adsorption chromatography (LAC) mode, polymers with identical repeating units, functionalities, and topology elute at the same retention time, independent of their molecular weight. The analysis of a block copolymer A-*block*-B at critical conditions of monomer A leads to elution volumes related to the segment B, whereas the segment A is chromatographically invisible. A LACCC dimension hyphenated with conventional SEC, i.e., two-dimensional or 2D chromatography, provides information on the chemical heterogeneity and size of the synthesized copolymers, respectively. It represents a useful tool for separation of copolymers from homopolymer residuals. In one example Matyjaszewski and coworkers[36] employed this characterization method to characterize linear and star-shaped copolymers synthesized via the ATRP polymerization technique. Furthermore, Falkenhagen and colleagues[37] characterized variable lengths of block copolymers synthesized via living anionic polymerization with 2D chromatography. Pasch et al.,[38] Wong et al.[39] and Inglis et al.[40] reported on the application of LACCC-SEC on block copolymers via coupling of functionalized homopolymers. Recently, Schmid et al.[41] used this chromatography technique for the characterization of block copolymers synthesized via combining RAFT polymerization with ring-opening polymerization (ROP). Further, copolymers based on macromonomers synthesized via conventional FRP were subjected to 2D chromatography by Müller and co-workers.[28,42,43]

The analysis of the statistical copolymers poly(BAMM)-*co*-poly(BzA) synthesized from BAMM with BzA via FRP should

evidence the copolymer structure of the samples as well as the quantity of potentially remaining—even after purification—homopolymer.

EXPERIMENTAL PART

Characterization. *Nuclear Magnetic Resonance (NMR).* NMR spectra of the synthesized copolymers were recorded on a Bruker AM 400 MHz spectrometer for hydrogen nuclei. Samples were dissolved in acetone-d_6. The solvent signal was used as an internal standard. Integration of the CH_2 (3) signal of the macromonomer was compared to the H_{ar} (2) and the CH_2 (1) signal of the benzyl acrylate, respectively, for copolymerization composition determination.

Size Exclusion Chromatography (SEC). SEC measurements were performed on a Polymer Laboratories PL-GPC 50 Plus Integrated System, comprising an autosampler and a PLgel 5 μm bead-size guard column (50 × 7.5 mm) followed by one PLgel 5 μm Mixed E column (300 × 7.5 mm), three PLgel 5 μm Mixed C columns (300 × 7.5 mm), and a differential refractive index detector using THF as the eluent at 35 °C with a flow rate of 1 mL min^{-1}. The SEC system was calibrated using linear poly(styrene) standards ranging from 160 to 6 × 10^6 g mol^{-1} (K = 14.1 × 10^{-5} dL g^{-1} and α = 0.70).[44] The resulting molecular weight distributions have been universally recalibrated using Mark−Houwink parameters for poly(butyl acrylate) (K = 12.2 × 10^{-5} dL g^{-1}, α = 0.70).[45] The concentration of the injected polymer solution was close to 2 mg mL^{-1}.

Size Exclusion Chromatography−Electrospray Ionization−Mass Spectrometry (SEC-ESI-MS). Mass spectra were recorded on a LXQ mass spectrometer (ThermoFisher Scientific) equipped with an atmospheric pressure ionization source operating in the nebulizer-assisted electrospray mode. The instrument was calibrated in the m/z range 195−1822 using a standard containing caffeine, Met-Arg-Phe-Ala acetate (MRFA), and a mixture of fluorinated phosphazenes (Ultramark 1621) (all from Aldrich). A constant spray voltage of 4.5 kV and a dimensionless sweep gas flow rate of 2 (~3 L min^{-1}) and a dimensionless sheath gas flow rate of 12 (~1 L min^{-1}) were applied. The capillary voltage, the tube lens offset voltage, and the capillary temperature were set to 60 V, 110 V and 275 °C, respectively. The solvent was a 3:2 v/v mixture of THF:methanol with polymer concentration ~0.2 mg mL^{-1}. The instrumental resolution of the employed experimental setup is 0.1 amu.

For SEC-ESI-MS the LXQ was coupled to a Series 1200 HPLC system (Agilent) that consisted of a solvent degasser (G1322A), a binary pump (G1312A), and a high performance autosampler (G1367B), followed by a thermostated column compartment (G1316A). Separation was performed on two mixed bed GPC columns (Polymer Laboratories, Mesopore 250 × 4.6 mm, particle diameter 3 μm) with precolumn (Mesopore 50 × 4.6 mm) operating at 30 °C. THF at a flow rate of 0.3 mL min^{-1} was used as the eluent. The mass spectrometer was coupled to the column in parallel to an RI detector (G1362A with SS420× A/D) in a setup described previously.[46] A 0.27 mL min^{-1} aliquot of the eluent was directed through the RI detector, and 30 μL min^{-1} infused into the electrospray source after postcolumn addition of a 0.1 mM solution of sodium iodide in methanol at 20 μL min^{-1} by a microflow HPLC syringe pump (Teledyne ISCO, Model 100DM). The polymer solutions (20 μL) with a concentration of 2 mg mL^{-1} were injected into the HPLC system.

Liquid Adsorption Chromatography under Critical Conditions (LACCC). The measurements of all copolymer samples were performed under the critical conditions of poly(BA) using an Agilent SECcurity SEC system (1200 series), comprising a degasser (G1379B), binary pump (G1312A), autosampler (G1329A) and a temperature controlling unit (G1316A), equipped with a normal phase column (EC 250/4.6 Nucleosil 300-5) at 35 °C. Detection was carried out with an evaporative light scattering detector (ELSD 400, SofTA Corp.). The flow rate of THF:n-hexane (28.7:71.3 v/v) eluent was set to 0.5 mL min^{-1}, and the samples were prepared in the mentioned eluent at a polymer concentration of 2 mg mL^{-1}, where 25 μL of the sample was injected. The copolymer samples were measured with a solvent gradient after the elution of residual macromonomer. Data acquisition and processing were accomplished with the PSS WinGPC Unity software package from Polymer Standards Service (PSS, Mainz, Germany) and the Agilent ChemStation for LC 3D Systems (Rev. B.04.01) from Agilent Technologies.

Materials. The monomers n-butyl acrylate (BA, Fluka, 99%) and benzyl acrylate (BzA, Alfa Aesar, 97%) were deinhibited by percolating over a column of activated basic alumina (Acros, Brockmann I, for chromatography, 50−200 μm) prior to use. Hexyl acetate (Acros, 99%) was used as received. The initiator 1,1′-azobis(isobutyronitrile) (AIBN, Sigma-Aldrich, 98%) was recrystallized twice from ethanol prior to use. 2-[(Dodecylsulfanyl)carbonothioyl]sulfanylpropanoic acid (DoPAT) is of a purity of >99% evidenced by nuclear magnetic resonance (NMR) and is obtained from Orica Pty Ltd., Melbourne, Australia, as a donation and used as received. Toluene (extra dry, water <30 ppm, Acros Organics), methanol (VWR, Prolabo, Normapur), tetrahydrofuran (multisolvent, 250 ppm BHT, Scharlau), and n-hexane (rotisolv, HPLC grade, Roth) were used as received.

Synthesis. *Synthesis of n-Butyl Acrylate Macromonomer (BAMM).* For the macromonomer synthesis n-butyl acrylate was polymerized with 5 × 10^{-3} mol L^{-1} AIBN in a 5 wt % solution of hexyl acetate (285 g, 1.98 mol) (freed from oxygen by purging with argon for about 40 min prior to the reaction) in a two-neck flask at 140 °C. The monomer (15.0 g, 0.12 mol, 5 wt %) was degassed by purging with argon for about 20 min in a separate vial sealed airtight with a septum at ambient temperature. The initiator AIBN (5 × 10^{-3} mol L^{-1}) was dissolved in hexyl acetate, freed from oxygen by purging with argon, and added to the reaction mixture at 140 °C. After 5 min the degassed monomer was added to the solvent. The reaction solution was subsequently stirred for about 10 h. After the reaction, the solvent was removed in a vacuum oven at 45 °C. The purity of the synthesized macromonomer was determined by size-exclusion chromatography (SEC) and electrospray ionization mass spectrometry (ESI-MS) (see Figures S1 and S2 in the Supporting Information). BAMM: M_n = 2300 g mol^{-1}, PDI = 1.90; the purity of BAMM exceeds 92% as estimated by ESI-MS (also refer to ref 20).

Copolymerization of n-Butyl Acrylate Macromonomer (Poly(BAMM)-co-poly(BzA)). For the synthesis of the copolymers poly(BAMM)-co-poly(BzA) variable mole fractions (0.1−0.9) of the monomer benzyl acrylate were used. The reaction preparation was performed in an inert gas atmosphere inside a glovebox. Benzyl acylate (f_{BzA}; 0.15 mol L^{-1} for f_{BzA} = 0.1 up to 1.21 mol L^{-1} for f_{BzA} = 0.9) was added to a solution of BAMM (f_{BAMM} = 1 − f_{BzA}; 1.33 mol L^{-1} for f_{BAMM} = 0.9 down to 0.13 mol L^{-1} for f_{BAMM} = 0.1) and AIBN (1 × 10^{-1} mol L^{-1}) in 1 mL of toluene with an Eppendorf pipette. The reaction mixture was then sealed airtight with a septum and stirred at 60 °C to a conversion of ~40%. The polymerization was stopped by cooling the mixture with liquid nitrogen. The solution was dried in a vacuum oven at 45 °C, and the residual monomer was removed. The resulting copolymer was recovered by precipitating the crude copolymer three times in an excess of cold methanol and then dried in vacuo. For a detailed analysis of the obtained statistical graft copolymers refer to the Results and Discussion section.

Synthesis of n-Butyl Acrylate Standards (Poly(BA)). Polymer standards for LACCC measurements were synthesized via the RAFT technique. The initial ratio of $[BA]_0$:$[DoPAT]_0$:$[AIBN]_0$ was 310:1:0.2. The reaction was performed at 60 °C for variable time intervals. The polymerization was stopped by cooling the mixture with liquid nitrogen. The residual monomer was subsequently removed in a vacuum oven at 45 °C. The polymers were analyzed via SEC and SEC-ESI-MS. The specifics for the four poly(BA) standards are as follows: poly(BA) 1: M_n = 8100 g mol^{-1}, PDI = 1.09; poly(BA) 2: M_n = 12 100 g mol^{-1},

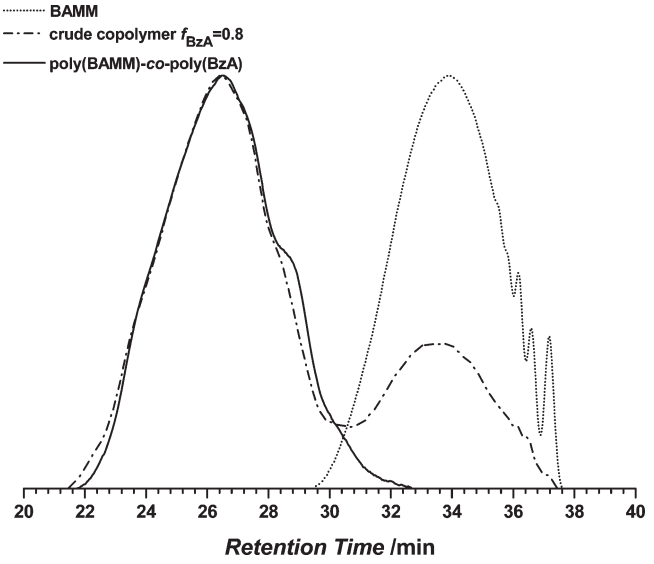

Figure 1. SEC elugrams of BAMM (dotted line), the crude product after the reaction (dashed line), and the copolymer (f_{BzA} = 0.8; straight line) after three times precipitation in an excess of cold methanol. Copolymerization conditions: BAMM, BzA, toluene, 1×10^{-1} mol L^{-1} AIBN, 60 °C, reaction time 1−3 h (depending on f_{BzA}), up to ∼40% conversion.

PDI = 1.06; poly(BA) 3: M_n = 19 000 g mol^{-1}, PDI = 1.04; poly(BA) 4: M_n = 24 600 g mol^{-1}, *PDI* = 1.04.

RESULTS AND DISCUSSION

Synthesis of the Copolymers. The determination of the copolymer structure of copolymers prepared during free radical polymerization of macromonomers synthesized via the high temperature acrylate polymerization with an acrylic monomer requires the synthesis of different copolymer samples. Thus, the copolymerization of BzA and BAMM was carried out for various initial comonomer feeds in solution of toluene with AIBN as a source of radicals. Polymerization in bulk is impractical due to diffusion restrictions associated with a decrease in the f_{BzA} fraction since the viscosity of the pure BAMM is relatively high. The addition of a solvent to the polymerization mixture of BzA and BAMM decreases viscosity. The mole fraction f_{BzA} was varied from 0.1 to 0.9 in 0.1 increments. After ∼40% conversion, determined gravimetrically, the copolymerization was stopped and residual macromonomer was removed from the crude copolymer by threefold precipitation in an excess of cold methanol. A typical SEC elugram of poly(BAMM)-*co*-poly(BzA) is shown in Figure 1.

The crude copolymer (dashed line) obtained from f_{BzA} = 0.8 displays a bimodal distribution (see Figure 1). Residual macromonomer (pure BAMM represented by the dotted line) appears at higher retention times, yet with reduced intensity. The residual BAMM comonomer is detectable in the crude poly(BAMM)-*co*-poly(BzA) due to incomplete conversion and needs to be eliminated. Three times precipitation of the crude product removes the residual macromonomer at higher retention times. Thus, the copolymer poly(BAMM)-*co*-poly(BzA) (represented by the straight line) exclusively shows a distribution at lower retention times, i.e., at higher molecular weights. The intensity of the residual macromonomer in the SEC elugrams of the crude

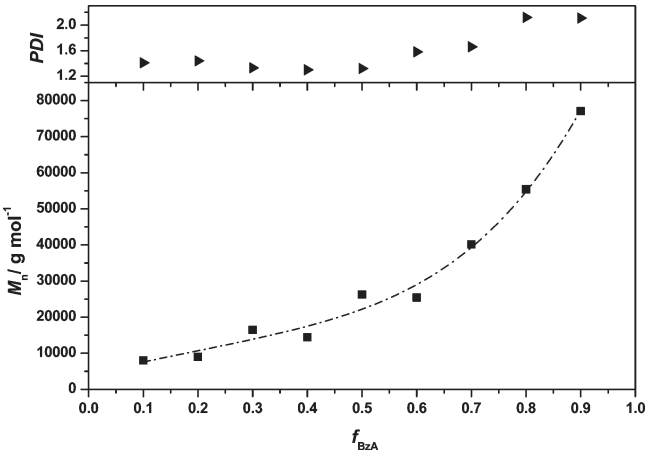

Figure 2. M_n (bottom) and *PDI* (top) as a function of the comonomer feed of benzyl acrylate f_{BzA} for the synthesized statistical copolymers poly(BAMM)-*co*-poly(BzA). Copolymerization conditions: BAMM, BzA, toluene, 1×10^{-1} mol L^{-1} AIBN, 60 °C, reaction time 1−3 h (depending on f_{BzA}), up to ∼40% conversion.

copolymer increases with a decrease in f_{BzA} (see Figure S3). A further precipitation is required for each sample to remove residual comonomer, resulting in a pure copolymer. Evidence for the complete removal of the macromonomer by precipitation was obtained from reference SEC measurements of polymer blends. To this end, benzyl acrylate homopolymer (poly(BzA)) has been synthesized via FRP with a molecular weight of M_n = 59 500 g mol^{-1} and mixed with BAMM in a certain ratio, i.e., 9:1 poly(BzA):BAMM. The resulting polymer blend BAMM-*blend*-poly(BzA) has been subjected to SEC. Even in a blend with 10% of BAMM (see Figure S4) the macromonomer is detectable at higher retention times. Since—after the precipitation step—the SEC elugrams show no residual distribution on the low molecular weight side, it is certain that no or if any only a minor amount of macromonomer (≪10%) remains within the copolymer sample.

The copolymers were analyzed via SEC using Mark−Houwink parameters for poly(BA) ($K = 12.2 \times 10^{-5}$ dL g^{-1}, α = 0.70).[45] The resulting values for molecular weight and polydispersity are shown in Figure 2.

The lower part of Figure 2 depicts the dependence of the number-average molecular weights (represented by the dashed line) on the mole fraction of f_{BzA} in the initial comonomer feed. With increasing mole fraction of benzyl acrylate, the molecular weight of the resulting copolymer increases; i.e., the copolymer obtained at f_{BzA} = 0.9 is close to a number-average molecular weight of 77 000 g mol^{-1} as the upper limit, whereas the copolymer generated at f_{BzA} = 0.1 has a number-average molecular weight of 8000 g mol^{-1} as lower limit. The polydispersity of the copolymers (upper part of Figure 2) lies in the range between 1.30 and 2.12 and increases with increasing f_{BzA}. The number-average molecular weights and *PDI*s of the copolymers have been determined using the Mark−Houwink parameters of poly(BA) homopolymers; thus, the values obtained via SEC analysis should be regarded as estimated values. The low *PDI*s appear as a consequence of the purification step, since low molecular weight copolymeric species are discriminated and removed simultaneously with the residual macromonomer. Inspection of Figure 2 suggests that the propagation rate and the probability of insertion of the macromonomer is significantly lower compared to that of benzyl acrylate. Such an observation is based on the resulting

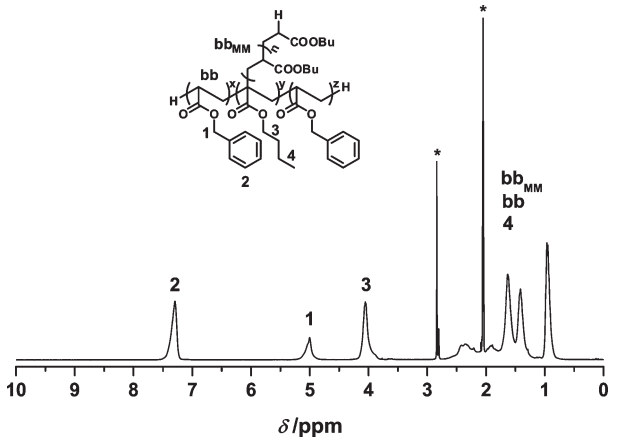

Figure 3. Typical 400 MHz ^{1}H NMR spectrum of poly(BAMM)-*co*-poly(BzA) (f_{BzA} = 0.8). The asterisks represent acetone and water in acetone, respectively. The structural formula with the detected resonances is inserted. Copolymerization conditions: BAMM, BzA, toluene, 1×10^{-1} mol L^{-1} AIBN, 60 °C, 3 h reaction time, up to ∼40% conversion.

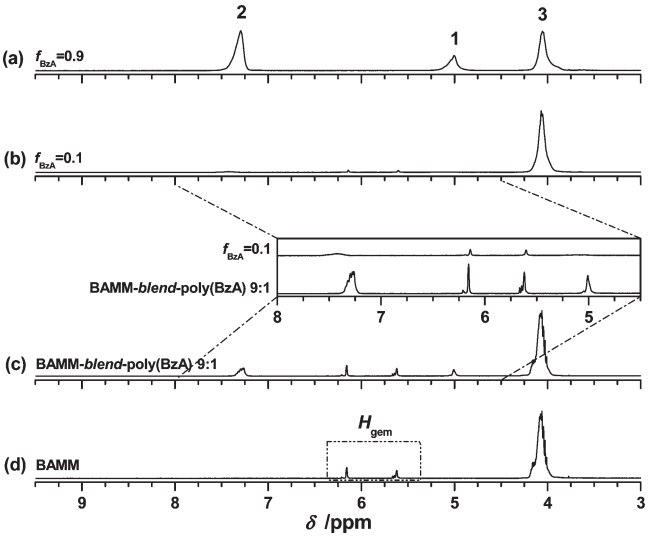

Figure 4. ^{1}H NMR spectra of (a) poly(BAMM)-*co*-poly(BzA) f_{BzA} = 0.9, (b) poly(BAMM)-*co*-poly(BzA) f_{BzA} = 0.1, (c) polymer blend BAMM-*blend*-poly(BzA) (9:1), and (d) BAMM. Copolymerization conditions: BAMM, BzA, toluene, 1×10^{-1} mol L^{-1} AIBN, 60 °C, 1 h (f_{BzA} = 0.9) and 3 h (f_{BzA} = 0.1) reaction time, up to ∼40% conversion. The inserted box displays the comparison of the copolymer synthesized at f_{BzA} = 0.1 and the BAMM-*blend*-poly(BzA) (9:1 wt %); note that the resonance CH_2 (3) of the macromonomer has been normalized for the spectra (2) and (3) in the inserted box; the polymeric signals H_{ar} (2) and CH_2 (1) of the BzA in the copolymer are less intense compared to the polymer blend due to different number-average molecular weights (8000 g mol^{-1} for the copolymer and 63 500 g mol^{-1} for the poly(BzA) of the polymer blend).

molecular weights at different mole fractions of comonomer BzA. The higher the comonomer feed of BzA in the comonomer mixture, the higher the achievable molecular weight. With a low f_{BzA} value only small amounts of BzA are present at the beginning of the polymerization which leads to lower molecular weights due to a potentially lower propagation rate of the macromonomer. In a subsequent step, the copolymer composition is determined.

Determination of Copolymer Composition. The determination of the copolymer composition for statistical copolymer obtained at variable initial BzA feed ratios, f_{BzA}, can open an avenue for a deeper understanding of the copolymerization process. For the determination of the copolymer composition, ^{1}H NMR spectra were recorded for polymers generated from experiments at variable mole fractions of the comonomer BzA. A typical ^{1}H NMR spectrum of a copolymer poly(BAMM)-*co*-poly(BzA) is depicted in Figure 3.

The assignments of the detected resonances are embedded in the structural formula within Figure 3. Benzyl acrylate was chosen as a comonomer due to the presence of an aromatic phenyl ring, which causes a broadened signal H_{ar} (2) at ∼7.3 ppm, representing the aromatic protons in the backbone benzyl ring, separated from other signals and the signal of CH_2 (1) at ∼5.01 ppm for the methylene protons next to the oxygen of the acrylic side chain. As a counterpart representative of the fraction of BA in the statistic copolymer, the signal for the methylene protons next to the oxygen (3) at ∼4.05 ppm in the side chain of the macromonomer was selected. The resonances in the region below 3 ppm are related to the protons of the polymer backbone, both benzyl acrylate and *n*-butyl acrylate macromonomer, and the alkyl chain of the *n*-butyl side chain of the macromonomer; these signals are not relevant for the copolymer composition determination and are thus not considered further. NMR spectra have been recorded for each prepared copolymer, and Figure 4 depicts the relevant NMR spectral region of the sample obtained for f_{BzA} = 0.9 (a) and f_{BzA} = 0.1 (b) as the upper and lower limits of the feed composition variation.

To evidence that the macromonomer has indeed undergone copolymerization, the following strategy is adapted: A ^{1}H NMR spectrum of a blend of 90 wt % BAMM and 10 wt % poly(BzA) is recorded and compared in the vinylic region to a copolymerization run of an initial ratio f_{BzA} = 0.1 and BAMM, respectively. If BAMM is indeed incorporated in a copolymer, a significant reduction in the geminal proton signal H_{gem} should be observed. Ideally, no geminal proton signal should remain in the copolymerization experiment. Spectrum (a) (top of Figure 4) depicts the case where f_{BzA} = 0.9. As it can be observed from spectrum (b), which represents f_{BzA} = 0.1, little residual macromonomer remains in the copolymer, as evidenced by the appearance of the resonances H_{gem} at ∼5.62 and ∼6.16 ppm for the geminal substituted olefine (pure BAMM is shown in spectrum (d)), featuring an f_{BzA} fraction of 0.3. Compared to the above-described SEC measurements, the NMR characterization shows a higher sensitivity due to the fact that residual BAMM is visible in the spectra having fractions below $f_{BzA} \leq 0.3$. With the decrease of the comonomer f_{BzA} the separation of the copolymer and residual BAMM by precipitation in cold methanol is becoming increasingly difficult. Nonetheless, copolymer is detectable as major product, evidenced by the appearance of signal CH_2 (1) and H_{ar} (2) of the benzyl acrylate comonomer, respectively. The ^{1}H NMR spectrum of a BAMM-*blend*-poly(BzA) (9:1) (c) evidence a substantial decrease of the vinylic proton resonances H_{gem} after the polymerization process in spectrum (b) since the intensity is much lower (∼72%) compared to the intensity in the spectrum of the polymer blend (c) (see inserted box of Figure 4). For the comparison of the spectrum of f_{BzA} = 0.1 (b) and the spectrum of the polymer blend (c) resonance CH_2 (3) of the macromonomer at ∼4.05 ppm has been normalized, hence the resonances H_{gem} in both spectra have been collated referring to

dx.doi.org/10.1021/ma201345m |*Macromolecules* 2011, 44, 6691–6700

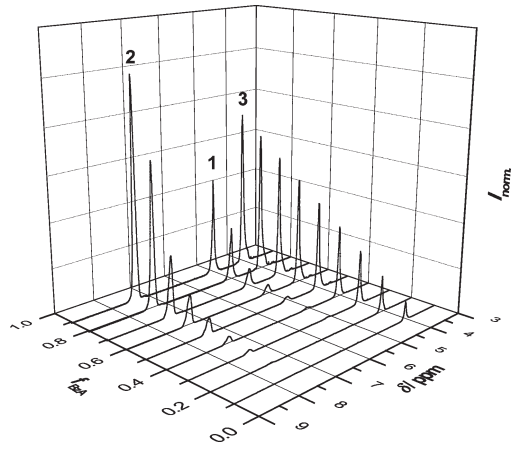

Figure 5. 3D ^{1}H NMR plot of poly(BAMM)-*co*-poly(BzA) copolymers synthesized at variable mole fractions f_{BzA}. Shown is the area from 3 to 9 ppm highlighting on the H_{ar} resonance of BzA (1), the CH_2 resonance of BzA (2), and CH_2 (3) resonance of BAMM.

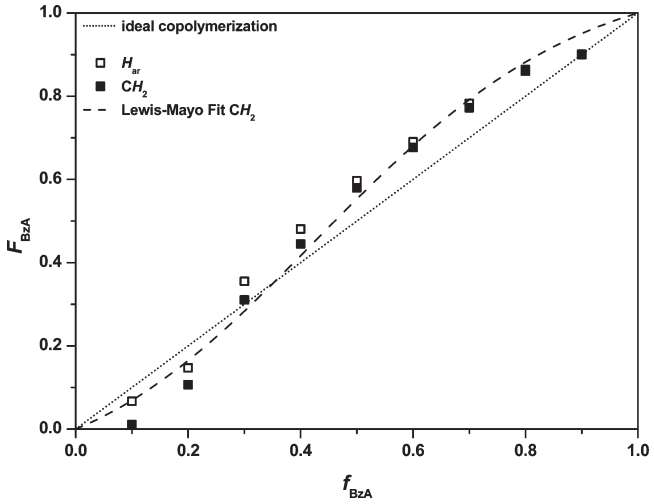

Figure 6. Mayo−Lewis plot for the entire copolymerization of BAMM with BzA in toluene with 1×10^{-1} mol L^{-1} AIBN at 60 °C to ∼40% of conversion determined gravimetrically. Values are determined from NMR integrals CH_2 (3) vs CH_2 (1) and H_{ar} (2), respectively. The derived reactivity ratios (see text) should be seen as estimated values.

their intensity. In addition, the decrease of the geminal resonances H_{gem} and the integral of CH_2 (3) confirms the incorporation of the comonomer BAMM in the copolymer. In the pure BAMM spectrum (d), the integrals of the resonance H_{gem}—compared to the integrals of the resonance CH_2 next to the oxygen in the acrylate moiety—are represented to be $2\,H : 4\,H \times [M_n(\mathrm{BAMM})/M(\mathrm{BA})]$. Taking into account that the resonance CH_2 (3) of the copolymer potentially represents both residual BAMM and BAMM grafted in the copolymer, the integral needs to be higher than the integral of the pure BAMM, which is associated with the measured copolymers.

For the relevant ppm area from 3 to 9 Figure 5 shows all ^{1}H NMR spectra from a mole fraction of 0.1 to 0.9 of BzA in the comonomer mixture in a three-dimensional plot. In Figure 5, the resonance of the methylene protons of the macromonomeric part CH_2 (3) have been normalized according to the comonomer feed f_{BzA} of the copolymerization mixture, i.e., the intensity of resonance (3) was set to 0.9 for the sample f_{BzA} = 0.9, the intensity of resonance (3) was set to 0.8 for the sample f_{BzA} = 0.8, etc. At high amounts of BzA, starting with f_{BzA} = 0.9, the intensity of both resonance (1) and (2) decrease with decreasing mole fraction of BzA. This implies that the resonances resulting from benzyl acrylate reduce with less available comonomer. A deeper understanding of the copolymers requires a more detailed consideration not only in terms of a qualitative observation of the signals but also the quantification of the integrals resulting from the relevant resonances, which characterize the copolymer.

For the determination of the copolymer composition F_{BzA}, both signals H_{ar} (2) and CH_2 (1) (BzA) were integrated and compared to the integral of signal CH_2 (3) associated with the amount of macromonomeric repeating units. The mole fraction F_{BzA} in the copolymer is given by eqs 2 and 3

$$F(\mathrm{BzA}) \frac{I(H_{ar\ BzA})}{\frac{2I(CH_{2\ BA})M(\mathrm{BA})}{M_n(\mathrm{BAMM})} + I(H_{ar\ BzA})} \quad (2)$$

$$F(\mathrm{BzA}) \frac{I(CH_{2\,BzA})}{\frac{I(CH_{2\ BA})M(\mathrm{BA})}{M_n(\mathrm{BAMM})} + I(CH_{2\,BzA})} \quad (3)$$

for the methylene protons CH_2 (1) of the acrylic side chain of the benzyl acrylate, respectively. In other words, the BAMM is treated as a monomer with a molecular weight close to M_n = 2300 g mol^{-1} (see Figures S1 and S2), i.e., a brush generating unit for the entire copolymer, whereas the benzyl acrylate generates a repeat unit of M = 162.19 g mol^{-1}. The polymerizable group of the BAMM represents the geminal 1,1′-disubstituted double bond as a pseudo-methacrylate, where the substituents are a *n*-butyl ester and the polymer backbone of the macromonomer. However, due to the fact that the macromonomer is present in the copolymer sample, the resonance CH_2 (3) displays the amount of macromonomeric repeating units in the copolymer as well as the residual macromonomer. Thus, the integral of resonance (3) has been reduced by the amount of residual macromonomer derived from the occurrence of the vinylic protons H_{gem}. Within the spectra the error obtained from residual macromonomer in the copolymer samples $f_{BzA} \leq 0.3$ is insignificant as the amount of residual comonomer reaches 1.64% at maximum for f_{BzA} = 0.1 as the highest amount of utilized macromonomer. The resulting values for the mole fraction in the copolymer F_{BzA} are plotted against the initial mole fraction f_{BzA} of the comonomer in the mixture. The resulting Mayo−Lewis plot is shown in Figure 6.

The hollow squares in Figure 6 represent the values determined from the aromatic resonances H_{ar} (2), whereas the filled squares are derived from the integration procedure involving the methylene resonances CH_2 (1) of the benzyl acrylate comonomer. It can be observed that the values F_{BzA} for H_{ar} are slightly higher compared to those derived from CH_2. This is caused by residual toluene in the samples after high vacuum overlapping with resonances of the H_{ar} (2) signal of the benzyl acrylate. Consequently, the values obtained from the resonances CH_2 (1) represent the copolymerization behavior of both monomers more accurately. Further, the calculation of the specific integrals from the measured ^{1}H NMR spectra—providing copolymer composition F_{BzA}—can be used for estimating the amount of grafted BAMM onto the copolymer backbone as a percentage of the overall molecular weight of the copolymer. The obtained

Table 1. Estimated *r* Values for the Copolymerization Process of BAMM with BzA in Toluene

	r_1 (r_{BzA}) (~40% conversion)	r_2 (r_{BAMM}) (~40% conversion)
H_{ar}[a]	2.12	1.26
CH_2	2.46	1.79

[a] Residual toluene in the samples overlapping with resonances of the H_{ar} (2) signal of the benzyl acrylate causes higher F_{BzA}; the values obtained from the resonances CH_2 (1) represent the copolymerization behavior of both monomers more accurately.

number-average molecular weights for each sample from f_{BzA} = 0.9 to f_{BzA} = 0.1 have been employed for a detailed analysis. The percentage of the grafted BAMM on the polymer backbone starts at ~0.78% for f_{BzA} = 0.9 and increases nearly linear up to 13.6% for f_{BzA} = 0.3. From f_{BzA} < 0.3, the amount of grafted BAMM increases rapidly up to 86.5% BAMM on the polymer backbone for f_{BzA} = 0.1 (see Figure S5).

In principle, the determination of the reactivity ratio of the copolymerization can be accomplished by further calculations based on the Mayo−Lewis equation (5). Various comonomer feeds f_{BzA} were applied to calculate reactivity ratios of the copolymer composition. Once the mole fraction F of one component in the copolymer mixture is determined, the values can be used in the Mayo−Lewis equation for copolymers:[25,47,48]

$$\frac{F_1}{F_2} = \frac{dc_{M_1}}{dc_{M_2}} = \frac{f_1(r_1 f_1 + f_2)}{f_2(r_2 f_2 + f_1)} \quad (4)$$

$$F_1 = \frac{r_1 f_1^2 + f_1 f_2}{r_1 f_1^2 + 2 f_1 f_2 + r_2 f_2^2} \quad (5)$$

with the mole fraction of component i in the monomer mixture f_i, the mole fraction of component i in the copolymer F_i, and the reactivity ratio $r_i = k_{pii}/k_{pjj}$. As eqs 4 and 5 are differential equations, the r values used to calculate the copolymer composition in a system with two monomers at indefinitely low conversions. However, the experiments were carried out to ~40% conversion due to precipitation restrictions of the copolymers at lower conversions. Thus, the reactivity ratios are calculated from the experimental composition data for an approximate estimation of the macromonomer reactivity in a free radical copolymerization with an acrylate; they are thus estimates, as it is clear that in the case of 100% conversion both values reach unity. However, experimental restrictions associated with polymer purification do not allow isolating copolymers at lower conversions. Fitting of the experimental data via the Mayo−Lewis equation (5) leads to the reactivity ratios of BAMM and BzA. The reactivity ratios originating from the NMR CH_2 (1) resonance (dashed line, Figure 6) and from the NMR H_{ar} (2) resonance are collated in Table 1. The dotted line embedded in Figure 6 represents ideal copolymerization behavior with $r_{i,j}$ = 1, meaning each monomer has the same addition probability to each propagation species, resulting in a statistical copolymer of a composition equal to the feed monomer ratio.

The integrals obtained from the aromatic resonances (2) are negligible, since aromatic protons of the residual toluene are counted additionally, leading to overestimated mole fractions in the copolymer feed. The resulting r values describe the system in a reasonable fashion, yet it needs to be clearly noted that the ratios have been calculated based on copolymers synthesized at ~40% conversion. Thus, the reactivity ratios represent an estimation; nevertheless, the values proof that the macromonomer synthesized via the high-temperature one-pot−one-step procedure undergoes copolymerization with small acrylate monomers. Interpretation of the calculated reactivity ratios—considering their estimated nature—leads to the following: r_1 = 2.46 represents the propagation tendency of benzyl acrylate. The radical character on a benzyl acrylate terminus of the copolymer prefers to propagate with the identical species, namely a benzyl acrylate monomer, whereas the same applies to the macromonomer, which propagates preferentially with itself resulting in r_2 = 1.79. When considering both reactivity ratios, the benzyl acrylate propagation step is favored. Such an observation may be associated with the steric demand of the macromonomer, especially if two BAMMs are placed next to each other within the copolymer. However, it is assumed that the lower molecular weight chains of the macromonomer (PDI = 1.90) potentially have a higher propagation probability due to decreased steric hindrance. In contrast, benzyl acrylate is sterically unambitious and shows a higher propagation rate related to the macromonomer. The understanding on a molecular level is correlated with the molecular weights (see Figure 2) achieved from the copolymerization process. The decrease of molecular weight with the decrease of f_{BzA} generates a low molecular weight copolymer due to lower propagation of the in excess present macromonomer and the low availability of the faster propagating benzyl acrylate in these samples. For f_{BzA} > 0.35, the Mayo−Lewis fit (dashed line) lies above ideal copolymerization (dotted line) and below the ideal for lower f_{BzA} content. The azeotropic point of the copolymer composition, where f_{BzA} equals F_{BzA}, is reached at approximately f_{BzA} = 0.35. The copolymerization of high-temperature acrylate polymerization macromonomers thus leads to statistic copolymers with benzyl acrylate monomers in the polymer backbone as well as grafted BAMM units, depending on the amount of macromonomeric repeat units in the copolymer.

It is additionally important to note that even though the (benzyl acrylate) radical chain terminus has a high propensity to add a monomeric acrylate monomer, addition of a BAMM unit is not much slower and the individual rate coefficient of addition is within a factor of 2−3 of the homopropagation rate of the acrylate. For the modeling of high-temperature acrylate polymerization, this rate coefficient was to date not known with sufficient certainty and while simulation results indicated fairly high addition rates of macromonomer units to growing chains,[19,49] no direct experimental data were available so far. The agreement between the copolymerization parameter of 2.46 determined herein and the value obtained by Hutchinson and colleagues for high-temperature homopolymerization of BA (1.82)[49] is—considering the indirect approach to determine the value via kinetic simulations—remarkable.

The copolymerization behavior of structurally very similar macromonomers and the estimation of their reactivity ratios have been studied before. Among others, Hirano et al. report in 2003 the free radical copolymerization of unsaturated oligomers (n = 2−4) of methyl acrylate with cyclohexyl acrylate.[50] They obtained reactivity ratios of the methyl acrylate tetramer of r_1 = 0.54 and r_2 = 0.96.[50] These dimer, trimers and tetramers for methyl acrylate featured the same olefinic terminus and should thus be expected to behave similar to the macromonomers under investigation in the present study. It could, however, be expected that the steric demand of these significantly smaller macromonomers

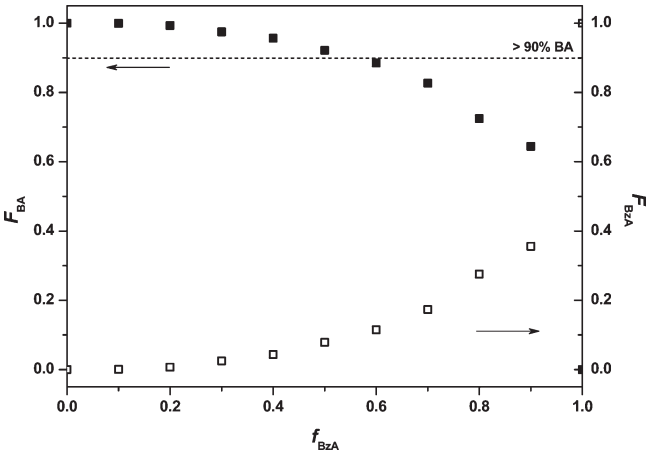

Figure 7. Visualization of the comonomer feed of BA (filled squares) and BzA units (hollow squares) in the copolymer against the comonomer feed of BzA in the comonomer mixture. The squares in the region above the dotted line represent ≥90% BA in the copolymer.

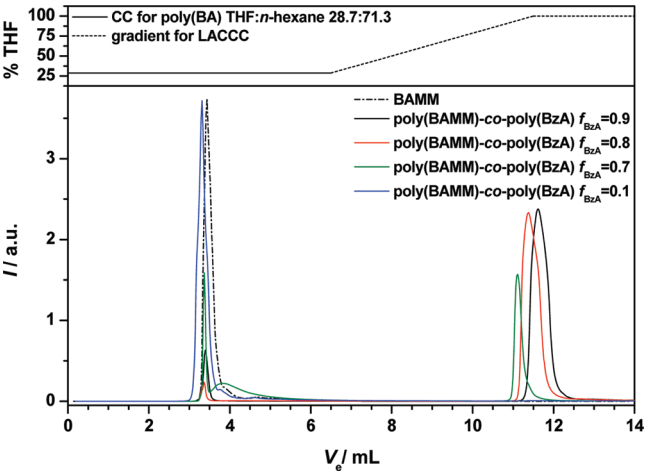

Figure 8. LACCC elugrams of different copolymer samples prepared at mole fractions 0.9 to 0.7 and 0.1 of BzA at critical conditions of poly(BA); the above inset shows the solvent gradient applied for the measurements on a normal phase column at 35 °C.

plays a significant role and may be responsible for the different reactivity (e.g., faster homopropagation of the macromonomers and increased propensity to add to an acrylate chain terminus). In light of this, it should be noted that the values determined herein represent an average over the whole distribution of macromonomer and that a chain-length dependency of the r values might exist.

In addition, Ohno et al. reported in 2006 that the reactivity ratios of macromonomers synthesized via postmodification of ATRP polymers of BA with BA are close to unity.[27] These parameters were, however, calculated from high conversion data; in this case it is not surprising that the reactivity ratios are close to unity since the parameters must reach unity for 100% conversion.

The above interpretation of the data is based on the treatment of the macromonomer as a comonomer, a view that underpins the calculations above and the Mayo−Lewis diagram. However, for a more detailed understanding, the copolymer needs to be analyzed in terms of its two monomeric constituents: *n*-butyl acrylate and benzyl acrylate. For each macromonomeric repeat unit in the final copolymer an average of ∼18 BA units (2300 g mol^{-1}/128.17 g mol^{-1}) are counted. Thus, the amount of BA is 18 times higher than the amount of benzyl acrylate related to the monomeric species. This fact is clarified in Figure 7, where the amount of BA and BzA units is plotted in contrast to Figure 6, where the macromonomer BAMM is considered as one constituent with ∼18 BA repeat units.

The amount of BA in the copolymer is represented by the filled squares, whereas the amount of BzA is represented by the hollow squares, respectively. A rapid increase from f_{BzA} = 1, which would yield a homopolymer with F_{BA} = 0, to f_{BzA} = 0.9 is visible in Figure 7 and reaches a BA copolymer composition of F_{BA} = 0.64. At a comonomer feed of f_{BzA} = 0.1 the percentage of incorporated benzyl acrylate is (almost) quantitative. The above analysis of the copolymer composition and its relation to the comonomer feed, in terms of the molecular building blocks, forms the basis for understanding the chromatographic results of the copolymer at critical conditions of poly(BA).

Chromatographic analysis of the statistical copolymers can offer a detailed understanding of the samples' composition. In principle, employing LACCC enables to assess the main part of the sample: the quantity of BAMM and BzA embedded in the copolymers. Such information can be more detailed than quantification via NMR as described above. When operated in 2D mode (thus in conjunction with size exclusion chromatography), separation for chemical composition as well as molecular weight is accessible, thus allowing to differentiate between copolymer of BzA and BAMM and the respective blend of homopolymers.

Characterization of the Copolymers by LACCC. Critical conditions for poly(BA) were determined and utilized to perform the analysis of the copolymers on a LACCC system. When measured on a high-pressure liquid chromatography system (HPLC) at 100% of a polymer soluble solvent—THF for poly(BA)—the copolymer samples elute according to their molecular weight in a narrow elution time window (see Figure S9, dashed line), whereas macromolecules can potentially be separated under critical conditions according to their composition (Figure S9, straight line for a copolymer sample and the dotted line for pure macromonomer). For that reason, poly(BA) standards with different molecular weights have been synthesized via reversible addition−fragmentation transfer polymerization (RAFT) (see Figure S6).[S1,S2] Under critical conditions of adsorption, the entropic and enthalpic effects between the polymer samples and the packing column are compensated. At the critical conditions of a specific polymer, the macromolecules elute at the same retention volume independent of their molar mass (see Figure S8). This implies that the first dimension (LACCC) separates no longer by size (SEC mode) but according to the chemical functionality. Critical conditions of poly(BA) on a normal phase column are realized at a solvent mixture of THF and *n*-hexane with a ratio of 28.7 to 71.3 (v/v) at 35 °C. The poly(BA) samples elute at a retention volume of around 3.38 mL regardless of their molecular weight. For a detailed graphical description of the critical conditions see Figures S7 and S8.

LACCC represents a useful tool for block copolymer characterization since the copolymers are separated according to their chemical functionality and the segment of the critical conditions gets invisible.[36−38] The LACCC measurement of the copolymers poly(BAMM)-*co*-poly(BzA) is applied to separate the various samples according to the incorporated amount of BzA in the polymer backbone analogous to the studies of Falkenhagen

et al.[37] However, the characterization of the statistic copolymers shows a different chromatographic behavior due to different macromolecular composition compared to block copolymers. For the measurement of the copolymers poly(BAMM)-*co*-poly(BzA) a solvent gradient was applied to reduce the measuring time (for 100% THF elugram see Figure S9). After 13 min of critical conditions the fraction of THF was allowed to reach 100% (over a period of 10 min) a condition that was applied for further 12 min. The utilized gradient is depicted in Figure 8 (top). After the elution volume of around 10−13 mL the actual copolymer is detectable. While separation of the polymers under critical conditions is possible, it should be noted that the elution volume for complete elution of the injected sample is fairly high. Thus, in order to apply size exclusion chromatography and to also assess the chain length of the eluted species (which requires a strong reduction in the flow rate of the HPLC dimension) unreasonably long retention times would be required and thus the analysis of the present copolymers had to be restricted to the LACCC mode.

Figure 8 shows LACCC elugrams of both the selected copolymers with a comonomer feed f_{BzA} of 0.9 to 0.7 and 0.1 and pure BAMM under critical conditions of poly(BA). The upper part of Figure 8 depicts the above-described gradient.

The copolymer samples appear to show residual macromonomer on the LACCC indicated by a distribution at the retention volume of poly(BA) (V_e = 3.23−3.81 mL) even for higher f_{BzA}. The samples elute in adsoption mode within the gradient and pure THF regime (V_e = 10.9−12.4 mL), which means that the copolymer produced at f_{BzA} = 0.9 (highest molecular weight) is detectable at higher retention volumes (V_e = 11.2−12.4 mL) than the copolymers prepared at f_{BzA} = 0.7 (V_e = 11.1−12.3 mL) and f_{BzA} = 0.8 (V_e = 10.9−11.8 mL). The copolymers elute depending on their molecular weight with increasing retention volume in ascending order. The elugrams appear to indicate that the amount of residual macromonomer (V_e = 3.23−3.81 mL) increases with the decrease of the mole fraction of BzA in the reaction mixture since the peak intensity increases with decreasing f_{BzA}. However, considering the amount of BA monomer units in the copolymers the signals at V_e = 3.23−3.81 mL can readily be understood as minor amounts of residual macromonomer, but even more important, additionally as copolymeric species with a considerable proportion of BA. As Figure 7 indicates, the amount of BA—for which critical conditions were applied—increases rapidly with decreasing amounts of BzA as each macromonomer—when incorporated in the copolymer—contributes ∼18 BA units. Even for the copolymer prepared at f_{BzA} = 0.9 the amount of BA lies above 60% and with the continuous increase of BAMM in the comonomer feed the incorporated BA in the copolymer reaches >90% for the copolymers synthesized at $f_{BzA} \leq 0.6$. Further, the amount of grafted BAMM on the polymer backbone increases for decreasing f_{BzA}—up to 86.5% BAMM on the polymer backbone for f_{BzA} = 0.1 (see Figure S5)—which indicates an excess of BA compared to BzA in the copolymer. In general, the analysis of a statistical copolymer is not necessarily depending on the end-group availability. In the case of a block copolymer, the elution behavior can easily be understood since block B represents a chain extension of the block A and the samples elute under critical conditions of A according to the length of block B. In the case of a statistic copolymer, as considered in the current study, A and B units are distributed over the entire copolymer. Since the mole fraction of BA in the copolymer is significantly higher compared to BzA (see Figure 7) and approximates 90% already at $f_{BzA} \leq 0.6$, the copolymers appear—at a certain ratio, which could be considered as a turning point—at the elution volume of pure poly(BA) homopolymer independent of their molecular weight on the LACCC. Thus, the high fraction of BA (>90% for samples prepared at $f_{BzA} \leq 0.6$) makes the copolymer chromatographically indistinguishable from the residual pure macromonomer. Thus, the copolymers could nearly be seen as a poly(BA) homopolymer with small defects induced by the incorporation of BzA in the polymer backbone. For $f_{BzA} \leq 0.6$ only one trace is detectable at V_e = 3.23−3.81 mL based on the previous explanation. For the sample f_{BzA} = 0.7 the turning point in LACCC behavior is clearly visible, displayed by the appearance of two distributions, one at higher elution volume (higher amount of F_{BzA}) and a second broadened trace in the BA area representing copolymers with small BzA repeat units as defects. In Figure 8, the copolymer sample resulting from f_{BzA} = 0.1 is shown as an example which contains F_{BzA} < 0.01 and elutes at the critical elution volume of poly(BA).

Since poly(BzA) homopolymer could potentially be formed during the copolymerization process as a side product, it is necessary to eliminate this doubt. Therefore, poly(BzA) homopolymer has been synthesized both via free radical and controlled radical polymerization (RAFT). However, the insolubility of poly(BzA) in the critical solvent mixture THF:*n*-hexane of the LACCC measurement removes poly(BzA) prior to the LACCC measurements. In conclusion, due to the insolubility of the homopolymer poly(BzA), the LACCC chromatograms in Figure 8 show the copolymeric species poly(BAMM)-*co*-poly(BzA).

CONCLUSIONS

In the current study *n*-butyl acrylate macromonomers synthesized via the high-temperature acrylate one-pot−one-step polymerization have been successfully copolymerized with benzyl acrylate as a representative acrylate monomer. Free radical copolymerization has been carried out for various comonomer feeds. The resulting statistic copolymers show a wide range in molecular weight depending on the initial mole fraction of the comonomer. The copolymer samples have been subjected to several characterization methods including SEC, NMR spectroscopy, and LACCC to obtain a detailed understanding of the generated structures. The integration of specific NMR resonances of the copolymer has been carried out. Further, composition analysis via the Mayo−Lewis equation provides estimates for the reactivity ratios of BAMM and BzA as comonomers. As the copolymerization has been carried out up to 40% conversion, the obtained reactivity ratio can be seen as estimates for the copolymerization. Generally, the obtained reactivity ratio is in overall good agreement with literature data on macromonomer addition to growing acrylate chains based on kinetic simulations. Furthermore, LACCC measurements under critical conditions of poly(BA) applied to the poly(BAMM)-*co*-poly(BzA) copolymers provide further proof for the formation of copolymeric material. It has thus been established that macromonomers prepared via the facile high-temperature synthesis approach featuring a broad molecular weight distribution can indeed copolymerize, rendering the synthesis of variable grafting density chain structures (depending on the initial mole fraction of f_{BzA}) a valuable tool for graft copolymer design.

■ ASSOCIATED CONTENT

Supporting Information. Further analytical data of BAMM, the poly(BA) standards and copolymers, and LACCC measurements. This material is available free of charge via the Internet at http://pubs.acs.org.

■ AUTHOR INFORMATION

Corresponding Author

*E-mail christopher.barner-kowollik@kit.edu, Tel +49 721 608 45641 (C.B.-K.). E-mail thomas.junkers@uhasselt.be, Tel +32 11 26 8318 (T.J.).

■ ACKNOWLEDGMENT

Financial support by the German Research Council (DFG) for the current work is gratefully acknowledged. C.B.-K. acknowledges additional funding for the current project from the Karlsruhe Institute of Technology (KIT) in the context of the Excellence Initiative for leading German universities as well as funding from the Ministry of Science and Arts of the state of Baden-Württemberg. The authors thank Christina Schmid for helpful discussions regarding the LACCC measurements.

■ REFERENCES

(1) Hadjichristidis, N.; Pitsikalis, M.; Iatrou, H.; Pispas, S. *Macromol. Rapid Commun.* **2003**, *24*, 979–1013.
(2) Li, D.; Grady, M. C.; Hutchinson, R. A. *Ind. Eng. Chem. Res.* **2005**, *44*, 2506–2517.
(3) Li, D.; Leiza, J. R.; Hutchinson, R. A. *Macromol. Theory Simul.* **2005**, *14*, 554–559.
(4) McHale, R.; Aldabbagh, F.; Carroll, W. M.; Yamada, B. *Macromol. Chem. Phys.* **2005**, *206*, 2054–2066.
(5) Quan, C. L.; Soroush, M.; Grady, M. C.; Hansen, J. E.; Simonsick, W. J. *Macromolecules* **2005**, *38*, 7619–7628.
(6) Yamada, B.; Zetterlund, P. B.; Sato, E. *Prog. Polym. Sci.* **2006**, *31*, 835–877.
(7) Matyjaszewski, K.; Xia, J. H. *Chem. Rev.* **2001**, *101*, 2921–2990.
(8) Schön, F.; Hartenstein, M.; Müller, A. H. E. *Macromolecules* **2001**, *34*, 5394–5397.
(9) Topham, P. D.; Sandon, N.; Read, E. S.; Madsen, J.; Ryan, A. J.; Armes, S. P. *Macromolecules* **2008**, *41*, 9542–9547.
(10) Chiefari, J.; Jeffery, J.; Mayadunne, R. T. A.; Moad, G.; Rizzardo, E.; Thang, S. H. *Macromolecules* **1999**, *32*, 7700–7702.
(11) Chiefari, J.; Moad, G.; Rizzardo, E.; Gridnev, A. A. US 98/47927, 1998.
(12) Willemse, R. X. E.; van Herk, A. M.; Panchenko, E.; Junkers, T.; Buback, M. *Macromolecules* **2005**, *38*, 5098–5103.
(13) Nikitin, A. N.; Hutchinson, R. A.; Buback, M.; Hesse, P. *Macromolecules* **2007**, *40*, 8631–8641.
(14) Junkers, T.; Bennet, F.; Koo, S. P. S.; Barner-Kowollik, C. *J. Polym. Sci., Part A: Polym. Chem.* **2008**, *46*, 3433–3437.
(15) Barner-Kowollik, C.; Davis, T. P.; Stenzel, M. H. *Polymer* **2004**, *45*, 7791–7805.
(16) Junkers, T.; Barner-Kowollik, C. *J. Polym. Sci., Part A: Polym. Chem.* **2008**, *46*, 7585–7605.
(17) Koo, S. P. S.; Junkers, T.; Barner-Kowollik, C. *Macromolecules* **2009**, *42*, 62–69.
(18) Junkers, T.; Koo, S. P. S.; Davis, T. P.; Stenzel, M. H.; Barner-Kowollik, C. *Macromolecules* **2007**, *40*, 8906–8912.
(19) Junkers, T.; Barner-Kowollik, C. *Macromol. Theory Simul.* **2009**, *18*, 421–433.
(20) Zorn, A.-M.; Junkers, T.; Barner-Kowollik, C. *Macromol. Rapid Commun.* **2009**, *30*, 2028–2035.
(21) Zorn, A.-M.; Malkoch, M.; Carlmark, A.; Barner-Kowollik, C. *Polym. Chem.* **2011**, *2*, 1163–1173.
(22) Grady, M. C.; Simonsick, W. J.; Hutchinson, R. A. *Macromol. Symp.* **2002**, *182*, 149–168.
(23) Cai, Y. L.; Hartenstein, M.; Muller, A. H. E. *Macromolecules* **2004**, *37*, 7484–7490.
(24) Krivorotova, T.; Vareikis, A.; Gromadzki, D.; Netopilik, M.; Makuska, R. *Eur. Polym. J.* **2010**, *46*, 546–556.
(25) Nguyen, S.; Marchessault, R. H. *Macromolecules* **2005**, *38*, 290–296.
(26) Norman, J.; Moratti, S. C.; Slark, A. T.; Irvine, D. J.; Jackson, A. T. *Macromolecules* **2002**, *35*, 8954–8961.
(27) Ohno, S.; Matyjaszewski, K. *J. Polym. Sci., Part A: Polym. Chem.* **2006**, *44*, 5454–5467.
(28) Roos, S. G.; Muller, A. H. E.; Matyjaszewski, K. *Macromolecules* **1999**, *32*, 8331–8335.
(29) Ryan, J.; Aldabbagh, F.; Zetterlund, P. B.; Yamada, B. *React. Funct. Polym.* **2008**, *68*, 692–700.
(30) Meijs, G. F.; Rizzardo, E. *J. Macromol. Sci., Rev. Macromol. Chem. Phys.* **1990**, *C30*, 305–377.
(31) Merz, E.; Alfrey, T.; Goldfinger, G. *J. Polym. Sci.* **1946**, *1*, 75–82.
(32) Fukuda, T.; Ma, Y. D.; Inagaki, H. *Macromolecules* **1985**, *18*, 17–26.
(33) Davis, T. P.; O'Driscoll, K. F.; Piton, M. C.; Winnik, M. A. *Polym. Int.* **1991**, *24*, 65–70.
(34) Coote, M. L.; Johnston, L. P. M.; Davis, T. P. *Macromolecules* **1997**, *30*, 8191–8204.
(35) Coote, M. L.; Zammit, M. D.; Davis, T. P.; Willett, G. D. *Macromolecules* **1997**, *30*, 8182–8190.
(36) Gao, H. F.; Min, K.; Matyjaszewski, K. *Macromol. Chem. Phys.* **2006**, *207*, 1709–1717.
(37) Falkenhagen, J.; Much, H.; Stauf, W.; Muller, A. H. E. *Macromolecules* **2000**, *33*, 3687–3693.
(38) Pasch, H. *Polymer* **1993**, *34*, 4095–4099.
(39) Wong, E. H. H.; Stenzel, M. H.; Junkers, T.; Barner-Kowollik, C. *Macromolecules* **2010**, *43*, 3785–3793.
(40) Inglis, A. J.; Barner-Kowollik, C. *Polym. Chem.* **2011**, *2*, 126–136.
(41) Schmid, C.; Falkenhagen, J.; Barner-Kowollik, C. *J. Polym. Sci., Part A: Polym. Chem.* **2011**, *49*, 1–10.
(42) Roos, S. G.; Müller, A. H. E.; Matyjaszewski, K. *Controlled/Living Radical Polymerization*; American Chemical Society: Washington, DC, 2000; Vol. 768, pp 361−371.
(43) Roos, S. G.; Schmitt, B.; Müller, A. H. E. *Polym. Prepr.* **1999**, *40*, 984.
(44) Strazielle, C.; Benoit, H.; Vogl, O. *Eur. Polym. J.* **1978**, *14*, 331–334.
(45) Penzel, E.; Goetz, N. *Angew. Makromol. Chem.* **1990**, *178*, 191–200.
(46) Gruendling, T.; Guilhaus, M.; Barner-Kowollik, C. *Anal. Chem.* **2008**, *80*, 6915–6927.
(47) Lewis, F. M.; Walling, C.; Cummings, W.; Briggs, E. R.; Mayo, F. R. *J. Am. Chem. Soc.* **1948**, *70*, 1519–1523.
(48) Mayo, F. R.; Lewis, F. M. *J. Am. Chem. Soc.* **1944**, *66*, 1594–1601.
(49) Wang, W.; Nikitin, A. N.; Hutchinson, R. A. *Macromol. Rapid Commun.* **2009**, *30*, 2022–2027.
(50) Hirano, T.; Zetterlund, P. B.; Yamada, B. *Polym. J.* **2003**, *35*, 491–500.
(51) Chiefari, J.; Chong, Y. K.; Ercole, F.; Krstina, J.; Jeffery, J.; Le, T. P. T.; Mayadunne, R. T. A.; Meijs, G. F.; Moad, C. L.; Moad, G.; Rizzardo, E.; Thang, S. H. *Macromolecules* **1998**, *31*, 5559–5562.
(52) Barner-Kowollik, C. *Handbook of RAFT Polymerization*; Wiley-VCH: Weinheim, 2008.